HHS Public Access

Author manuscript

Mov Disord. Author manuscript; available in PMC 2017 August 10.

Published in final edited form as:

Mov Disord. 2017 January ; 32(1): 124–133. doi:10.1002/mds.26834.

[18F]AV-1451 tau-PET in progressive supranuclear palsy

Jennifer L. Whitwell, PhD[1], **Val J. Lowe, MD**[1], **Nirubol Tosakulwong, BS**[2], **Stephen D. Weigand, MS**[2], **Matthew L. Senjem, MS**[1,3], **Christopher Schwarz, PhD**[1], **Anthony J. Spychalla, BS**[1], **Ronald C. Petersen, MD, PhD**[4], **Clifford R. Jack Jr, MD**[1], and **Keith A. Josephs, MD, MST, MSc**[4]

[1]Department of Radiology, Mayo Clinic, Rochester, MN, USA

[2]Department of Health Sciences Research, Mayo Clinic, Rochester, MN, USA

[3]Department of Information Technology, Mayo Clinic, Rochester, MN, USA

[4]Department of Neurology, Mayo Clinic, Rochester, MN, USA

Abstract

Background—The [18F]AV-1451 positron emission tomography ligand allows the in-vivo assessment of tau proteins in the brain. It shows strong binding in Alzheimer's dementia but little is known about how it performs in progressive supranuclear palsy, a primary 4R tauopathy.

Objectives—To determine whether [18F]AV-1451 uptake can be observed in progressive supranuclear palsy and to characterize the regional distribution compared to controls and Alzheimer's dementia.

Corresponding author: Jennifer L. Whitwell, PhD, Department of Radiology, Mayo Clinic, 200 1st St SW, Rochester, MN 55905, Tel: 507-284-5576, Fax: 507-284-9778, Whitwell.jennifer@mayo.edu.

Financial disclosures: The authors have no conflicts of interest

Author roles
Conception and design of the study: JW, KJ
Statistical analysis: NT, SW
Acquisition and analysis of data: VL, MS, CS, AS, RP, CJ
Writing the first draft of the manuscript: JW, KJ
Review and critique of manuscript: VL, NT, SW, MS, CS, AS, RP, CJ

Financial Disclosures of all authors
Stock Ownership in medically-related fields: CJ owns stock in Johnson & Johnson.
Intellectual Property Rights: None
Consultancies: RP is a consultant for Roche, Inc., Merck, Inc., Genentech, Inc., Biogen, Inc., and Eli Lilly and Co. CJ has provided consulting services for Eli Lilly.
Expert Testimony: None
Advisory Boards: VL serves on scientific advisory boards for Bayer Schering Pharma and Piramal Life Science. RP serves on data monitoring committees for Pfizer, Inc. and Janssen Alzheimer Immunotherapy.
Employment: None
Partnerships: None
Contracts: None
Honoraria: None
Royalties: RP receives publishing royalties from Mild Cognitive Impairment (Oxford University Press, 2003)
Grants: JW was supported by NIH grants R01-DC12519, R01-NS89757, R01-AG050603, and R01-AG37491-06. VL was supported by grants from the NIH, GE Healthcare, Siemens Molecular Imaging, and AVID Radiopharmaceuticals. RP was supported by NIH grants P50-AG016574, U01 AG006786, and R01 AG034676. CJ was supported by NIH grants R01-AG11378 and R01-AG041851 and the Alexander Family Alzheimer's Disease Research Professorship of the Mayo Foundation. KJ was supported by NIH grants R01-DC12519, R01-NS89757, R01-AG050603, and R01-AG37491-06.

Methods—[^{18}F]AV-1451 positron emission tomography was performed in ten patients with probable progressive supranuclear palsy. These patients were age and gender-matched to 50 controls and ten Alzheimer's dementia patients that had undergone identical [^{18}F]AV-1451 imaging. Regional comparisons of [^{18}F]AV-1451 uptake were performed across the whole brain using region-of-interest and voxel-level analyses, and correlations between regional [^{18}F]AV-1451 and the progressive supranuclear palsy rating scale were assessed.

Results—An elevated [^{18}F]AV-1451 signal was observed in progressive supranuclear palsy compared to controls in pallidum, midbrain, dentate nucleus of the cerebellum, thalamus, caudate nucleus, and frontal regions. Signal in the cerebellar dentate and pallidum were also greater in progressive supranuclear palsy compared to Alzheimer's dementia. Conversely, [^{18}F]AV-1451 signal across the cortex was higher in Alzheimer's dementia compared to progressive supranuclear palsy. [^{18}F]AV-1451 signal in a number of regions correlated with the progressive supranuclear palsy rating scale.

Conclusions—Progressive supranuclear palsy is associated with elevated [^{18}F]AV-1451 signal in a characteristic and distinct regional pattern that correlates with disease severity and differs from the patterns observed in Alzheimer's dementia.

Keywords

Tau; positron emission tomography; progressive supranuclear palsy; Alzheimer's dementia

Introduction

Progressive supranuclear palsy (PSP) is a neurodegenerative tauopathy characterized by the deposition of 4-repeat (4R) tau in globose neurofibrillary tangles, tufted astrocytes, coiled bodies and threads that are found in basal ganglia, diencephalon, brainstem and motor and premotor cortex[1, 2]. The most common clinical phenotype associated with PSP is Richardson's syndrome, characterized by difficulty with gait and postural instability, frequent falls, and abnormal eye movements (vertical supranuclear gaze palsy)[3, 4]. Tau is a major target for future treatments of PSP, and a number of clinical treatment trials of therapies targeting tau are already underway and recruiting patients with Richardson's syndrome. Unfortunately, however, the assessment of tau severity and distribution in PSP during life has not been possible due to the absence of a tau biomarker. Traditional pathological examinations of tau burden suffer from the limitations that very small sections of tissue are sampled and only one half of the brain is typically sampled limiting the evaluation of distribution across the whole brain.

Positron emission tomography (PET) ligands, such as [^{18}F]AV-1451, have recently been developed that specifically target tau proteins in the brain[5, 6]. This ligand was originally developed and optimized to target tau proteins present in Alzheimer's disease and the ligand shows strong medial temporal and cortical binding in patients with Alzheimer's dementia[7, 8]. However, this development also opens up exciting possibilities for the in vivo assessment of tau pathology in PSP. Tau-PET imaging could allow the assessment of the distribution of tau pathology, spread of tau pathology over time, and the assessment of how tau pathology is associated with clinical measures collected at the same point in time.

Understanding the natural biology of tau deposition in PSP will ultimately be critical to determine how tau-PET measurements should be used as outcome measures for treatment trials and to aid diagnosis. However, an essential first step is to determine how tau-PET imaging behaves in patients with PSP.

The aim of our study was to assess tau-PET imaging using [^{18}F]AV-1451 in a group of PSP patients to determine whether uptake can be observed compared to age matched healthy control subjects, and to characterize the regional distribution of tau-PET uptake in PSP. We also aimed to determine whether [^{18}F]AV-1451 signal correlated to clinical disease severity at the time of tau-PET imaging, and how the regional distribution in PSP compares to the distribution in subjects with amnestic Alzheimer's dementia.

Methods

Subjects

Ten patients that fulfilled clinical criteria for probable PSP[3] underwent tau-PET imaging for this study. All patients with PSP that were evaluated in the Department of Neurology, Mayo Clinic, between February 20th 2015 and May 26h 2016 were consecutively recruited into an NIH-funded prospective longitudinal PSP study by a neurodegenerative specialist and PSP expert (KAJ). Patients were included in the study if they met criteria for probable PSP, had symptoms for ≤5 years and were able to ambulate independently. Patients meeting criteria for possible PSP[3], progressive akinesia with gait freezing[9], or PSP parkinsonism[10] were excluded from the study. All patients underwent clinical and neurological examination and completed standardized and validated testing. All PSP patients completed the PSP rating scale (PSPRS)[11] as a measure of clinical disease severity and the Montreal Cognitive Assessment (MoCA)[12] as a measure of global cognitive function.

The 10 PSP patients were matched by age and gender to 50 healthy control subjects (30 (60%) female, median (IQR) age=65 (59–69) years) using a 5:1 matching scheme. All 50 healthy controls had been recruited into the Mayo Clinic Study of Aging and had undergone identical tau-PET imaging with [^{18}F]AV-1451 between May 14th 2015 and April 20th 2016. In addition, the PSP patients were matched by age and gender to 10 patients meeting clinical criteria for amnestic Alzheimer's dementia[13] using a 1:1 matching scheme. The Alzheimer's dementia cohort were 6 (60%) female, with median (IQR) age=66 (63–73) years, age at onset=63 (56–65) years), disease duration=6 (3.9–8.3) years, and Mini-Mental state Examination score[14]=23 (21–24). All Alzheimer's dementia patients had been recruited into the Mayo Clinic Alzheimer's Disease Research Center and had undergone identical tau-PET imaging with [^{18}F]AV-1451 between April 7th 2015 and March 10th 2016.

The study was approved by the Mayo IRB. All subjects consented to research.

Tau-PET analysis

Tau-PET imaging was performed using the [^{18}F]AV-1451 ligand. PET scans were acquired using a 690 XT PET/CT scanner (GE Healthcare, Milwaukee, Wisconsin) operating in 3D mode. An intravenous bolus injection of approximately 370MBq (10mCi) of [^{18}F]AV-1451 was administered, followed by a 20 minute PET acquisition performed 80 minutes after

injection. Emission data was reconstructed into a 256×256 matrix with a 30-cm FOV (Pixel size=1.0mm, slice thickness=1.96mm). All subjects had a 3T MPRAGE sequence performed on the same day as the tau-PET. Partial volume correction (PVC) of PET data was performed using a two-compartment model[15].

[^{18}F]AV-1451 images were co-registered to the subjects MPRAGE using 6-degree-of-freedom rigid body registration. A modified version of the automated anatomical labeling atlas[16] was transformed into the native space of each MPRAGE and used to calculate regional [^{18}F]AV-1451 uptake in the grey and white matter. Median [^{18}F]AV-1451 uptake was calculated for 49 regions-of-interest (ROIs) including regions in the central grey matter, posterior fossa, medial and lateral frontal lobe, medial and lateral temporal lobe, parietal lobe and occipital lobe. Our analysis was purposefully broad in order to allow the assessment of the entire brain. A region-of-interest outlining the dentate nucleus of the cerebellum was manually drawn on the atlas using a T2*-weighted template for reference. Voxels containing the dentate nucleus of the cerebellum were removed from all other cerebellar regions-of-interest. Left and right hemisphere structures were combined for each ROI. Median [^{18}F]AV-1451 uptake in each ROI was divided by median uptake in cerebellar crus grey matter to create standard uptake ratios (SUVRs). There was no difference in raw [^{18}F]AV-1451 binding in the cerebellar crus across the disease groups (p=0.69 using Kruskal-Wallis Rank Sum Test, median [IQR] values in PSP=2590 [2120–2990], controls=2720 [2070–3210], AD=2910 [2460–3130]).

Voxel-level group comparisons of the [^{18}F]AV-1451 was also performed using SPM5. All MPRAGE scans were spatially normalized to a customized template[17] and segmented using the unified segmentation model[18], followed by the hidden Markov random field clean-up step. The [^{18}F]AV-1451 images were co-registered to the subject's MPRAGE using 6 degrees-of-freedom registration. The AAL atlas was propagated to native MPRAGE space. All voxels in the [^{18}F]AV-1451 image were divided by median uptake in cerebellar crus grey matter to create SUVR images. These images were then normalized to the customized template using the normalization parameters from the MPRAGE normalization. Voxel-level comparisons were performed using two-sided T-tests in SPM5, with results assessed at $p<0.05$ after correction for multiple comparisons using the false discovery rate correction. Age and gender were included in the analysis as covariates.

Statistics

For the ROI-level analysis, differences in the 49 ROIs between PSP and both controls and Alzheimer's dementia were tested using two-sample Wilcoxon/Mann-Whitney tests and summarized by the area under the receiver operating characteristic curve (AUROC) which can be interpreted as a nonparametric measure of effect size, i.e. group-wise differences, independent of the underlying scale of measurement. In general, the higher the AUROC estimates, the better the discrimination between groups. These analyses were not adjusted for multiple comparisons since adjustment would increase the type II errors for associations that are not null. Not adjusting for multiple comparisons has been advocated since it will result in fewer errors in interpretation when the data are not random numbers but actual observations on nature[19]. Adjusting our data could therefore result in missing important

findings, particularly in this exploratory analysis. We note that in the SPM5 analysis we use false discovery rate correction because of the large scale of the hypothesis testing. We also performed partial correlation analyses using Spearman rank correlations adjusted for age and gender between PSPRS and tau SUVr values in regions where the p-values from the two-sample Wilcoxon/Mann-Whitney tests between PSP and controls were less than 0.05. Our analyses were performed using PVC tau-PET images, as well as repeated using non-PVC tau-PET images; given that it is currently unclear which method is the most appropriate for tau-PET imaging[7, 8]. All analyses were performed with R statistic software (version 3.1.3; R Foundation for Statistical Computing, Vienna, Austria).

Results

Demographics

The median age at onset for all 10 PSP subjects was 63 years (range: 57–65), median age at examination 65 years (range: 60–69) and median disease duration 3.5 years (range: 2.5–4.0). Six of the 10 PSP subjects were female (60%). At the time of [^{18}F]AV-1451 tau-PET all PSP patients were essentially cognitively intact with a median MoCA score of 27 (range: 25–30), and all were of moderate severity with a median PSPRS score of 37 (range: 32–39).

PSP compared to controls

In the ROI-level analysis, elevated tau-PET signal was observed in the PSP patients compared to controls in the midbrain, pallidum, thalamus, supplementary motor area, dentate nucleus of the cerebellum, precentral cortex, frontal inferior opercularis, caudate nucleus and middle frontal gyrus (Figure 1). Of these regions, only the pallidum, dentate nucleus of the cerebellum, thalamus and midbrain showed significantly elevated signal in PSP compared to controls in the non-PVC comparison.

In the voxel-level analysis, the PSP group showed elevated tau-PET signal bilaterally in the dentate nucleus of the cerebellum, midbrain, thalamus, subthalamic nucleus, pallidum, caudate nucleus and supplementary motor areas, compared to controls (Figure 2). All regions, except for the supplementary motor area, were also identified in the non-PVC comparison.

Individual tau-PET images from the 10 PSP patients are shown in Figure 3. Some variability was observed across PSP patients, although most patients showed greater SUVRs in dentate nucleus of the cerebellum, midbrain, thalamus, subthalamic nucleus, and basal ganglia, compared to cortical regions. Elevated SUVRs in these regions was also observed in some of the healthy controls (Figure 3).

PSP compared to Alzheimer's dementia

In the ROI-level analysis (Figure 4), median tau-PET signal was greater in PSP compared to Alzheimer's dementia in the dentate nucleus of the cerebellum, pallidum, midbrain, thalamus and pons, although the only differences to reach significance were the dentate nucleus of the cerebellum and the pallidum. The tau-PET signal in all of the rest of the ROIs was greater in Alzheimer's dementia than in the PSP, with the most striking difference

observed in medial and lateral parietal regions. These results were the same in the non-PVC comparisons.

In the voxel-level analysis (Figure 2), the PSP group showed greater tau-PET signal in midbrain, dentate nucleus of the cerebellum, thalamus and pallidum compared to Alzheimer's dementia. The Alzheimer's dementia group showed greater tau-PET signal throughout the temporoparietal, frontal and occipital cortices compared to controls and PSP. These results were the same in the non-PVC comparisons. Widespread cortical tau-PET signal can be seen in the two Alzheimer's dementia patients shown in Figure 3.

PSPRS correlations in PSP

Correlations were identified between PSPRS scores and [^{18}F]AV-1451 uptake in midbrain (r=0.78, p=0.02), thalamus (r=0.76, p=0.027), dentate nucleus of the cerebellum (r=0.74; p=0.037), precentral cortex (r=0.77, p=0.02), supplementary motor area (r=0.73, p=0.04), middle frontal gyrus (r=0.75, p=0.03), and frontal inferior opercularis (r=0.64, p=0.06) (Figure 5). Correlations were also observed in the non-PVC data between all these regions and the PSPRS, except for the middle frontal gyrus and frontal inferior opercularis. The PSPRS scores did not correlate with [^{18}F]AV-1451 uptake in pallidum (r=0.20, p=0.64) or caudate nucleus (r=0.27, p=0.51), either with or without PVC.

Discussion

We demonstrated that elevated [^{18}F]AV-1451 signal was observed in PSP patients compared to age-matched controls. The pattern of elevated signal was relatively focal, involving pallidum, dentate nucleus of the cerebellum, midbrain, thalamus, caudate nucleus and frontal lobe; all regions which typically show tau deposition at autopsy in PSP.

The regional [^{18}F]AV-1451 signal elevation in PSP was particularly striking in subcortical, cerebellar and brainstem regions compared to controls and would be consistent with a recently published case report, that also found elevated [18F]AV-1451 uptake in PSP, largely in the pallidum and midbrain[20]. These regions also showed greater signal in PSP compared to the Alzheimer's dementia patients, suggesting a distinct pattern specific for PSP, at least when compared to Alzheimer's dementia and controls. However, it should be noted that increased signal in these regions may be difficult to identify in individual PSP patients because many of these subcortical structures showed age-associated elevated signal in the healthy control subjects (Figure 3), as others have noted[8, 21]. Our group-level analysis controlled for this confounder by comparing our PSP patients to healthy controls and Alzheimer's dementia patients that were well matched by age, and our PSP patients indeed showed higher signal than what would be expected for their age. The overlap still observed between PSP and the age-matched controls would, however, likely limit the diagnostic value of these regional [^{18}F]AV-1451 measures in individual patients. In addition to the focal pattern of subcortical tau-PET signal, we did observe involvement of some cortical regions, particularly the supplementary motor area and middle and inferior frontal lobes. However, these regions only showed significant signal increase in the analysis that utilized partial volume correction; no cortical regions were identified in the images that had not been corrected for partial volume averaging. It is, therefore, possible that the presence of atrophy

in the frontal lobe reduced the tau-PET signal in the raw images. The alternative explanation would be that the partial volume correction over inflated signal in regions that lie close to the cerebrospinal fluid boundary, such as cortical regions and the caudate nucleus. Further work will be needed to analyze the value of partial volume correction in tau-PET data. Nevertheless, it is clear that the cortical signal was less than that observed in subcortical, brainstem and cerebellar regions. The majority of the cortical regions did not survive correction for multiple comparisons in the voxel-level analyses, either with or without partial volume correction, and would likely not survive correction at the region-level. This may suggest that tau pathology spreads from subcortical regions to cortex; although longitudinal studies will be needed to investigate this hypothesis.

Greater tau-PET signal in the dentate nucleus of the cerebellum, midbrain, thalamus, supplementary motor area and inferior and middle frontal gyri also correlated with greater impairment on the PSPRS in the PSP subjects. The presence of tau pathology in these regions may, therefore, be particularly important for the development of the clinical features of PSP. This adds to data from previous studies that have shown a relationship between neurodegeneration of the dentatorubrothalamic white matter tract[22] and connectivity in the supplementary motor area, and disease severity in PSP[23, 24]. The dentatorubrothalamic tract connects the dentate nucleus of the cerebellum to the thalamus via the midbrain, with projections from the thalamus then terminating in the premotor cortex. We could, therefore, hypothesize that the clinical features of PSP may develop as a result of a breakdown in this functional network of regions along the dentatorubrothalamic tract[22], which in turn may result from the deposition of tau in these regions. We could also hypothesize that the lack of correlations with PSPRS in the basal ganglia structures may be because these regions are not central to this dentatorubrothalamic network. A note of caution, however, is that the correlations would be affected by inclusion of different PSP clinical variants, as well as the spread of disease severities present in the cohort.

Both the subcortical and cortical regions identified in this study do typically show neurodegeneration and tau pathology at autopsy[2, 25]. However, we must be cautious in the pathological interpretation of these tau-PET findings. Recent autoradiographic studies have shown little binding of [^{18}F]AV-1451 to 4R tau in autopsy samples from cases of PSP, compared to striking binding to 3R+4R tau in autopsy samples from cases of Alzheimer's dementia[21, 26, 27]. Our findings are not inconsistent with this, given that the magnitude of binding (i.e. SUVr's) in the individual PSP patients was relatively low compared to the striking uptake observed in the cortex in the patients with Alzheimer's Dementia. These findings are consistent with either the ligand being more specific to the 3+4R isoform that characterizes Alzheimer's disease associated tau than the 4R tau isoform that characterizes PSP, or the ligand being more specific to paired helical filaments associated with Alzheimer's dementia versus straight filaments associated with PSP[21, 27]. Another possibility for the difference in uptake could be the relative amount of mature vs early neurofibrillary tangles that are present in Alzheimer's disease vs PSP; Alzheimer's disease having a higher ratio of mature/early tangles compared to PSP. Regardless of the exact reason, it appears that AV-1451 does bind to some 4R tau, although it is likely only binding a small fraction of the total 4R tau burden in PSP. Studies assessing the correlation between [^{18}F]AV-1451 binding on antemortem PET and the severity of 3R+4R tau at autopsy have

been performed[28], but more work is needed to assess the specificity of [^{18}F]AV-1451 in autopsy confirmed PSP patients that have undergone [^{18}F]AV-1451 tau-PET imaging during life.

Although some mild [^{18}F]AV-1451 uptake was observed in cortical regions in PSP, the degree of cortical uptake was higher in Alzheimer's dementia compared to PSP across all cortical ROIs, but particularly in medial and lateral parietal regions. Elevated cortical uptake in Alzheimer's dementia agrees with previous studies[7, 8, 29]. Perhaps surprisingly, we observed higher SUVr values in the neocortex compared to medial temporal lobe regions, particularly the hippocampus, in our Alzheimer's dementia cohort. This may, however, reflect the young age of our Alzheimer's dementia cohort, since greater tau deposition in the cortex compared to the hippocampus at autopsy has been associated with younger age in Alzheimer's disease[30, 31]. A similar predominance of cortical uptake compared to the hippocampus has been observed in a tau-PET study using [^{18}F]AV-1451 that also had a relatively young Alzheimer's dementia cohort[8], and another tau-PET study found a greater cortical burden in young-onset compared to old-onset Alzheimer's dementia[7].

A strength of our study is the homogeneity of the cohort, with all patients presenting with Richardson's syndrome, the most common variant of PSP, and all fulfilling criteria for probable PSP. A diagnosis of probable PSP has a high sensitivity and specificity for pathological PSP[32, 33]. Our findings may not, however, generalize to patients with other clinical variants of PSP, or to PSP patients with a different degree of disease severity. Given the weak binding of [^{18}F]AV-1451 to 4R tau in PSP in autoradiographic studies, and the lack of other published PET studies on [^{18}F]AV-1451 in PSP, we must be cautious in drawing conclusions about the utility of this ligand in diagnosis, or as a biomarker, in PSP. Our data shows that it may hold some promise as a research tool, although a ligand with more robust binding may be more ideal. There are also some potential issues with the [^{18}F]AV-1451 ligand to consider. One issue is the fact that elevated signal in some of the PSP-related structures, such as basal ganglia, midbrain and dentate nucleus of the cerebellum, can also be seen in healthy controls, and may be related to the presence of iron pigment or neuromelanin[21]. Another issue to take into account is that [^{18}F]AV-1451 off-target binding to neuromelanin[27] could be reduced when compared to controls due to the loss of pigmented dopaminergic neurons in the midbrain in PSP, similar to what has been shown in Parkinson's disease[34]. The difference observed between PSP and both controls and Alzheimer's dementia in the midbrain may, therefore, have been reduced due to these issues. These factors ultimately limit the diagnostic specificity of [^{18}F]AV-1451 signal in these regions to PSP. Other tau PET ligands are also available that may prove to be useful in PSP[35, 36], although validation of these ligands in patients with PSP, and PSP brain tissue, and comparison to [^{18}F]AV-1451, is required.

Despite these issues, this study demonstrates that PSP does show elevated signal on tau-PET imaging with [18F]AV-1451 in a characteristic and distinct regional pattern that correlates with disease severity.

Acknowledgments

Funding sources: The study was funded by R01-NS89757, P50-AG016574, U01 AG006786, and R01 AG034676

The study was funded by R01-NS89757, P50-AG016574, U01 AG006786, and R01 AG034676. We would like to acknowledge AVID Radiopharmaceuticals for provision of AV-1451 precursor, chemistry production advice and oversight, and FDA regulatory cross-filing permission and documentation needed for this work.

References

1. Hauw JJ, Daniel SE, Dickson D, et al. Preliminary NINDS neuropathologic criteria for Steele-Richardson-Olszewski syndrome (progressive supranuclear palsy). Neurology. 1994; 44(11):2015–2019. [PubMed: 7969952]
2. Dickson, DW., Hauw, JJ., Agid, Y., Litvan, I. Progressive Supranuclear Palsy and Corticobasal Degeneration. In: Dickson, D., Weller, RO., editors. Neurodegeneration: The molecular pathology of dementia and movement disorders. 2. Chichester, UK: Wiley-Blackwell; 2011.
3. Litvan I, Agid Y, Calne D, et al. Clinical research criteria for the diagnosis of progressive supranuclear palsy (Steele-Richardson-Olszewski syndrome): report of the NINDS-SPSP international workshop. Neurology. 1996; 47(1):1–9. [PubMed: 8710059]
4. Steele JC, Richardson JC, Olszewski J. Progressive Supranuclear Palsy. a Heterogeneous Degeneration Involving the Brain Stem, Basal Ganglia and Cerebellum with Vertical Gaze and Pseudobulbar Palsy, Nuchal Dystonia and Dementia. Archives of neurology. 1964; 10:333–359. [PubMed: 14107684]
5. Chien DT, Bahri S, Szardenings AK, et al. Early clinical PET imaging results with the novel PHF-tau radioligand [F-18]-T807. Journal of Alzheimer's disease : JAD. 2013; 34(2):457–468. [PubMed: 23234879]
6. Xia CF, Arteaga J, Chen G, et al. [(18)F]T807, a novel tau positron emission tomography imaging agent for Alzheimer's disease. Alzheimer's & dementia : the journal of the Alzheimer's Association. 2013; 9(6):666–676.
7. Cho H, Choi JY, Hwang MS, et al. Tau PET in Alzheimer disease and mild cognitive impairment. Neurology. 2016
8. Johnson KA, Schultz A, Betensky RA, et al. Tau positron emission tomographic imaging in aging and early Alzheimer disease. Annals of neurology. 2016; 79(1):110–119. [PubMed: 26505746]
9. Williams DR, Holton JL, Strand K, Revesz T, Lees AJ. Pure akinesia with gait freezing: a third clinical phenotype of progressive supranuclear palsy. Mov Disord. 2007; 22(15):2235–2241. [PubMed: 17712855]
10. Williams DR, de Silva R, Paviour DC, et al. Characteristics of two distinct clinical phenotypes in pathologically proven progressive supranuclear palsy: Richardson's syndrome and PSP-parkinsonism. Brain. 2005; 128(Pt 6):1247–1258. [PubMed: 15788542]
11. Golbe LI, Ohman-Strickland PA. A clinical rating scale for progressive supranuclear palsy. Brain. 2007; 130(Pt 6):1552–1565. [PubMed: 17405767]
12. Nasreddine ZS, Phillips NA, Bedirian V, et al. The Montreal Cognitive Assessment, MoCA: a brief screening tool for mild cognitive impairment. Journal of the American Geriatrics Society. 2005; 53(4):695–699. [PubMed: 15817019]
13. McKhann GM, Knopman DS, Chertkow H, et al. The diagnosis of dementia due to Alzheimer's disease: recommendations from the National Institute on Aging-Alzheimer's Association workgroups on diagnostic guidelines for Alzheimer's disease. Alzheimer's & dementia : the journal of the Alzheimer's Association. 2011; 7(3):263–269.
14. Folstein MF, Folstein SE, McHugh PR. "Mini-mental state". A practical method for grading the cognitive state of patients for the clinician. Journal of psychiatric research. 1975; 12(3):189–198. [PubMed: 1202204]
15. Meltzer CC, Kinahan PE, Greer PJ, et al. Comparative evaluation of MR-based partial-volume correction schemes for PET. J Nucl Med. 1999; 40(12):2053–2065. [PubMed: 10616886]

16. Tzourio-Mazoyer N, Landeau B, Papathanassiou D, et al. Automated anatomical labeling of activations in SPM using a macroscopic anatomical parcellation of the MNI MRI single-subject brain. NeuroImage. 2002; 15(1):273–289. [PubMed: 11771995]
17. Vemuri P, Whitwell JL, Kantarci K, et al. Antemortem MRI based STructural Abnormality iNDex (STAND)-scores correlate with postmortem Braak neurofibrillary tangle stage. NeuroImage. 2008; 42(2):559–567. [PubMed: 18572417]
18. Ashburner J, Friston KJ. Unified segmentation. NeuroImage. 2005; 26(3):839–851. [PubMed: 15955494]
19. Rothman KJ. No adjustments are needed for multiple comparisons. Epidemiology. 1990; 1(1):43–46. [PubMed: 2081237]
20. Hammes J, Bischof GN, Giehl K, et al. Elevated in vivo [18F]-AV-1451 uptake in a patient with progressive supranuclear palsy. Mov Disord. 2016
21. Lowe VJ, Curran G, Fang P, et al. An autoradiographic evaluation of AV-1451 Tau PET in dementia. Acta Neuropathol Commun. 2016; 4(1):58. [PubMed: 27296779]
22. Whitwell JL, Avula R, Master A, et al. Disrupted thalamocortical connectivity in PSP: a resting-state fMRI, DTI, and VBM study. Parkinsonism Relat Disord. 2011; 17(8):599–605. [PubMed: 21665514]
23. Agosta F, Galantucci S, Svetel M, et al. Clinical, cognitive, and behavioural correlates of white matter damage in progressive supranuclear palsy. Journal of neurology. 2014; 261(5):913–924. [PubMed: 24599641]
24. Whitwell JL, Master AV, Avula R, et al. Clinical correlates of white matter tract degeneration in progressive supranuclear palsy. Archives of neurology. 2011; 68(6):753–760. [PubMed: 21670399]
25. Schofield EC, Hodges JR, Macdonald V, Cordato NJ, Kril JJ, Halliday GM. Cortical atrophy differentiates Richardson's syndrome from the parkinsonian form of progressive supranuclear palsy. Mov Disord. 2011; 26(2):256–263. [PubMed: 21412832]
26. Sander K, Lashley T, Gami P, et al. Characterization of tau positron emission tomography tracer [F]AV-1451 binding to postmortem tissue in Alzheimer's disease, primary tauopathies, and other dementias. Alzheimer's & dementia : the journal of the Alzheimer's Association. 2016
27. Marquie M, Normandin MD, Vanderburg CR, et al. Validating novel tau positron emission tomography tracer [F-18]-AV-1451 (T807) on postmortem brain tissue. Annals of neurology. 2015; 78(5):787–800. [PubMed: 26344059]
28. Smith R, Puschmann A, Scholl M, et al. 18F-AV-1451 tau PET imaging correlates strongly with tau neuropathology in MAPT mutation carriers. Brain. 2016
29. Scholl M, Lockhart SN, Schonhaut DR, et al. PET Imaging of Tau Deposition in the Aging Human Brain. Neuron. 2016; 89(5):971–982. [PubMed: 26938442]
30. Murray ME, Graff-Radford NR, Ross OA, Petersen RC, Duara R, Dickson DW. Neuropathologically defined subtypes of Alzheimer's disease with distinct clinical characteristics: a retrospective study. Lancet Neurol. 2011; 10(9):785–796. [PubMed: 21802369]
31. Whitwell JL, Dickson DW, Murray ME, et al. Neuroimaging correlates of pathologically defined subtypes of Alzheimer's disease: a case-control study. Lancet Neurol. 2012; 11(10):868–877. [PubMed: 22951070]
32. Josephs KA, Petersen RC, Knopman DS, et al. Clinicopathologic analysis of frontotemporal and corticobasal degenerations and PSP. Neurology. 2006; 66(1):41–48. [PubMed: 16401843]
33. Respondek G, Roeber S, Kretzschmar H, et al. Accuracy of the National Institute for Neurological Disorders and Stroke/Society for Progressive Supranuclear Palsy and neuroprotection and natural history in Parkinson plus syndromes criteria for the diagnosis of progressive supranuclear palsy. Mov Disord. 2013; 28(4):504–509. [PubMed: 23436751]
34. Hansen AK, Knudsen K, Lillethorup TP, et al. In vivo imaging of neuromelanin in Parkinson's disease using 18F-AV-1451 PET. Brain. 2016; 139(Pt 7):2039–2049. [PubMed: 27190023]
35. Dani M, Brooks DJ, Edison P. Tau imaging in neurodegenerative diseases. Eur J Nucl Med Mol Imaging. 2016; 43(6):1139–1150. [PubMed: 26572762]

36. Maruyama M, Shimada H, Suhara T, et al. Imaging of tau pathology in a tauopathy mouse model and in Alzheimer patients compared to normal controls. Neuron. 2013; 79(6):1094–1108. [PubMed: 24050400]

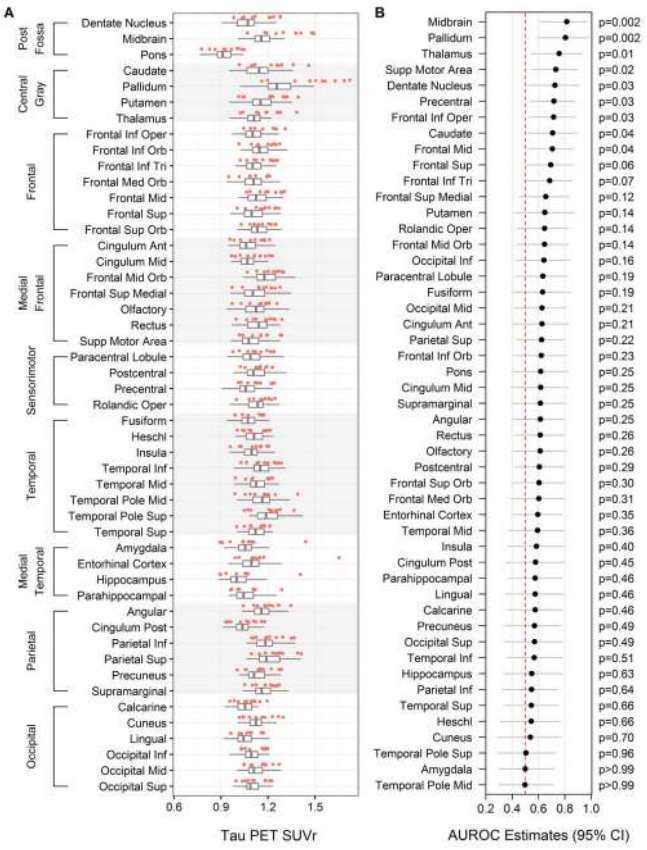

Figure 1.

Region-of-interest level comparison of PSP and healthy controls. Panel A shows box-plots of the distribution of tau SUVr values of 50 controls and red dots represent the 10 PSP subjects. Panel B shows estimated (95% CI) AUROCs between PSP and controls, ranked from the highest to the lowest. In the box-plots, the upper whisker extends from the hinge to the highest value that is within 1.5 * IQR of the hinge, where IQR is the inter-quartile range, or distance between the first and third quartiles. Inf = inferior, Mid = middle, Sup = superior, tri = triangularis, oper = opercularis, orb = orbital, ant = anterior, post = posterior

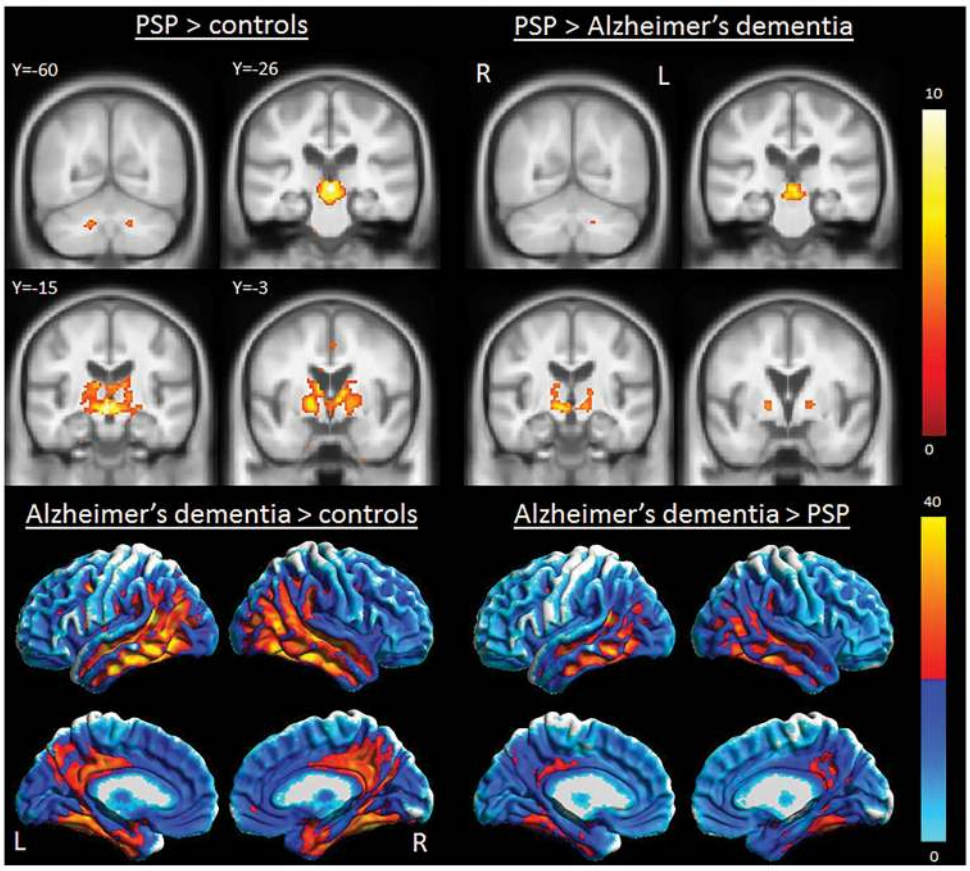

Figure 2.

Voxel-level group comparisons of tau-PET uptake. Regions that a showed greater signal in PSP compared to controls and Alzheimer's dementia are shown on coronal slices through the template (with Y coordinates provided), and regions that showed greater uptake in Alzheimer's dementia are shown on three dimensional renderings of the brain. Results are shown after PVC and corrected for multiple comparisons at $p<0.05$ using the false discovery rate correction.

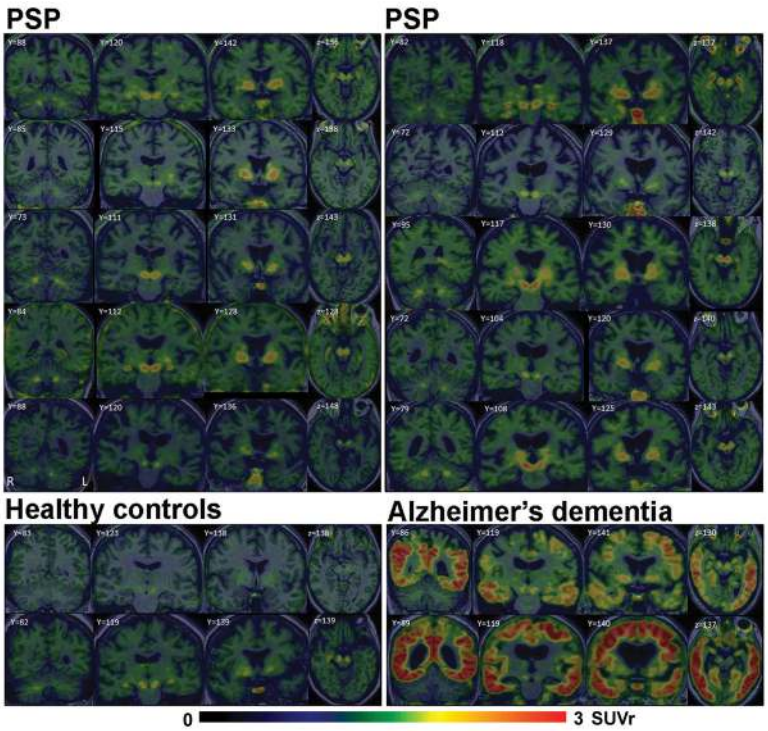

Figure 3.

Individual tau-PET images for the 10 PSP patients, two healthy controls and two Alzheimer's dementia patients. Coronal images at the level of the dentate nucleus of the cerebellum, midbrain and basal ganglia, as well as an axial image at the level of the midbrain, are shown. All images are shown on the same SUVr scale (0–3).

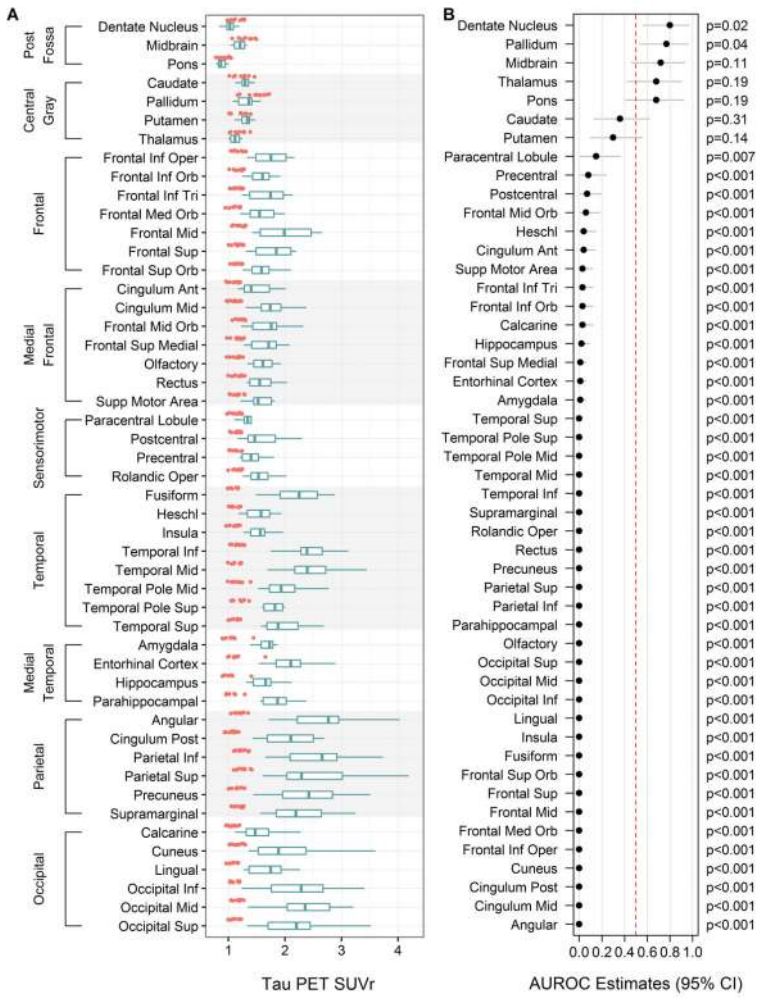

Figure 4.

Region-of-interest level comparison of PSP and Alzheimer's dementia. Panel A shows box-plots of the distribution of tau SUVr values of 10 Alzheimer's dementia patients (shown in blue) and red dots represent the 10 PSP subjects. Figure B shows estimated (95% CI) AUROCs between PSP and Alzheimer's dementia, ranked from the highest to the lowest. In the box-plots, the upper whisker extends from the hinge to the highest value that is within 1.5 * IQR of the hinge, where IQR is the inter-quartile range, or distance between the first and third quartiles. Inf = inferior, Mid = middle, Sup = superior, tri = triangularis, oper = opercularis, orb = orbital, ant = anterior, post = posterior

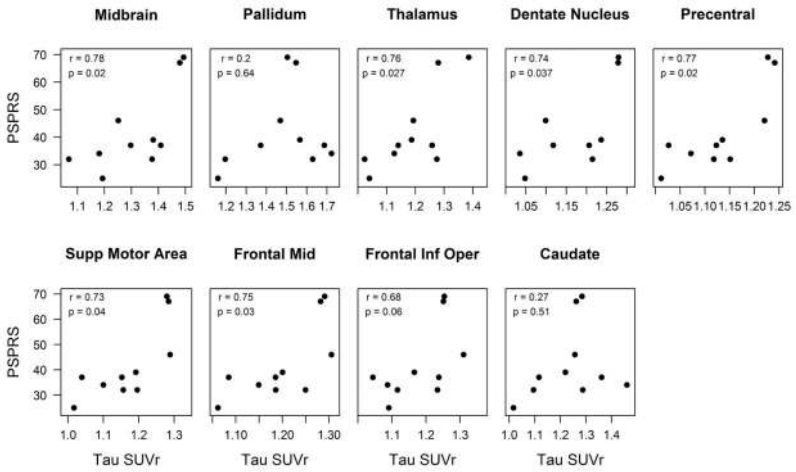

Figure 5.

Scatterplots between PSP rating scales and tau SUVr values with partial correlation estimates and p-value. Inf = inferior, Mid = middle, oper = opercularis